A parallel algorithm for step- and chain-growth polymerization in Molecular Dynamics

Pierre de Buyl^{1, 2} and Erik Nies¹

¹⁾ Division of Polymer Chemistry, Department of Chemistry, Katholieke Universiteit Leuven, Celestijnenlaan 200F, B-3001 Heverlee, Belgium

²⁾SIM vzw, Technologiepark 935,BE-9052 Zwijnaarde, Belgium

We propose a parallel algorithm for step- and chain-growth polymerization in the context of Molecular Dynamics simulations and present its implementation in the ESPResSo++ simulation software. The algorithm is based on a generic reaction scheme that is parametrized for step- and chain-growth, works at a given intrinsic rate and produces continuous trajectories. For chain growth, our results are compared to the existing simulation literature. For step growth, a rate equation is presented for the evolution of the crosslinker population that compares well to the simulations for low crosslinker functionality.

I. INTRODUCTION

For many applications in soft-matter research, chemical bonds can be considered a given data that does not change in the course of time. For instance, the chemical structure of water is typically not modified in a molecular simulation when it is used as a solvent¹. Likewise, the structure and chemical bonds of complex molecules are typically fixed in the course of a simulation.

Creating new chemical bonds in a molecular simulation is a problem for which no general solution exists. This is due to the inherent complexity of the problem at hand, as chemical reactions are not part of the Hamiltonian mechanics paradigm that serves as the basis for classical Molecular Dynamics (MD) simulations. Several solutions have been proposed in the past, either for MD^{2,3} or for mesoscopic hydrodynamical models^{4,5}. No solution exists however for MD that supports a parallel programming model to simulate bond formation.

A completely different kind of simulation framework, ReaxFF⁶ is worth noting for reference. ReaxFF builds on ab initio data to reproduce the interactions in a dynamical approach: the parameters for the interatomic force fields are updated at each step to resemble those of a full quantum simulation. The creation and destruction of chemical bonds is a built-in benefit of this approach. It does not allow yet to simulate systems as large a classical MD allows.

In the present article, we focus on coarse grained models for the simulation of polymer systems. Their simplicity, in comparison to atomistic models, allows us to devise a consistent polymerization procedure. We consider only distance-dependent pairwise interactions between the particles that participate in the chemical reaction. The algorithm is exposed in full details and is implemented in the ESPResSo++ soft-matter simulation software⁷ as an extension that is distributed as part of the version 1.9. The execution of the algorithm makes use of the Message Passing Interface for distributed memory parallel computing, which ESPResSo++ already uses.

The algorithm manages chain- and step-growth mechanisms. Simulations for both mechanisms are presented and the time-evolution of the crosslinking process is com-

pared to rate equations.

II. BOND FORMATION MODEL AND ALGORITHM

A single bonding algorithm, set with appropriate parameters, can be used to generate different growth mechanisms. We describe this general algorithm, present its implementation and its application to the step- and chain-growth mechanisms for polymerization. We introduce a state variable for all particles that will define their active and/or available status. It is denoted by

$$A^{s*}, (1)$$

where s is the state of the particle A. This variable was not present in ESPResSo++ but its addition was straightforward thanks to the modular nature of the software. Only irreversible reactions are considered here.

The creation of bonds is ruled by the chemical equation

$$T^{t*} + A^{a*} \xrightarrow{k} T^{(t+\delta t)*} - A^{(a+\delta a)*}$$
 (2)

that represents the behaviour of a target T and an active particle A. Before the reaction, T and A have no specific connection besides the nonbonded excluded volume interaction. T and A particles in a given interaction range will react at a rate k, if they meet criteria detailed in the following of the text, to form a connected compound T-A. The state of T and A is then updated according to the reaction parameters δt and δa .

The criteria for reaction are: (i) The species of the particles in the pair must match T and A. In the case of a homopolymer, A and T may be the same. (ii) The state of T must be equal to 0. (iii) The state of A must be greater than a given minimum s_{min}^A . This will be used to assign a given functionality to A.

The formation of bonds proceeds as follows: (i) Find all pairs that satisfy the above criteria. (ii) Store the pairs after testing their acceptance based on the rate k. (iii) Collect the pairs from step (ii) across neighboring CPUs. (iv) Execute the change of states and modify the interaction. The implementation of the procedure is given in Sec. III.

In order to avoid discontinuities in the trajectories or in the energy of the simulated system, the bonded interaction must not impact the particle at the time of the reaction. This is achieved by using a bonded potential that is equal to zero below a given cut-off following the proposition by Akkermans et al². A consequence is that the reaction is thermoneutral and that thermostatting is not required to absorb energy jumps as in previous studies^{3,8}. To the authors' knowledge, controlled exoor endothermic reaction schemes for MD do not exist.

At variance with Akkermans et al², however, the rate of the reaction is not controlled by the interval at which the reaction is performed (τ_r in Ref. 2). Instead, it is the value of k that dictates the dynamics. Reactions are performed every Θ MD steps of timestep Δt (see Sec. III) and the parameters must obey

$$k \, \Delta t \, \Theta \ll 1 \ .$$
 (3)

A pair is considered for reaction if

$$u < k \, \Delta t \, \Theta \,$$
, (4)

where u is a random number distributed uniformly in [0,1). The random number in ESPResSo++ is uniform_01 from the Boost C++ Libraries⁹.

A. Chain growth

Chain growth is considered to occur at the single active end of a polymer chain of n units

$$P_{n-1} - P^* + M \xrightarrow{k} P_n - P^*$$
 (5)

so that the monomer M becomes the last, and active, unit of the polymer chain. Here, P* is the *active* particle and M the *target* particle. While there is a single active unit in a polymer chain, there may be many polymer chains in a single simulation. Every unit, except the first and last in a chain, may form two bonds: one as the target and one as the active particle. The units are thus of functionality two.

The kinetic evolution of the population of chains is given, following Akkermans $et \ al^2$ by

$$[\dot{P}_1] = -k_c[M][P_1],$$
 (6a)

$$[P_{n+1}] = -k_c[M]([P_{n+1}] - [P_n]),$$
 (6b)

where the dot denotes the time derivative. The effective rate constant for the chains $k_c = k\rho^{-1}\langle N_{P^*M}\rangle$ takes into account the intrinsic rate k and the average number $\langle N_{P^*M}\rangle$ of available monomers M around a polymer end-unit P*. Following Ref. 2, $\langle N_{P^*M}\rangle$ is considered independent of the chain length and is obtained from simulations in which the polymerization is stopped. [·] stands for the number density (or concentration) of a given particle type and has the units of an inverse volume.

As a consequence of Eqs. (6), the average concentration of monomers [M] follows a simple evolution:

$$[\dot{M}] = -k_c[M] \sum_{n=1}^{\infty} [P_n] \tag{7}$$

$$= -k_c[M][P^*] \tag{8}$$

where $[P^*]$ is the concentration of active end-units, which is a constant here. The resulting concentration of monomers thus follows an exponential decay

$$[M](t) = [M_0]e^{-k_c[P^*]t} , (9)$$

where $[M_0]$ is the initial value of the concentration [M]. Alternatively, we may consider the polymer fraction

$$\phi(t) = 1 - \frac{[M](t)}{[M] + [P] + [P^*]}$$

$$= 1 - \frac{[M_0]}{[M] + [P] + [P]^*} e^{-k_c[P^*]t}$$

$$\approx 1 - e^{-k_c[P^*]t}, \qquad (10)$$

where the approximation accounts for the fact that almost all particles in the system are available monomers at the beginning of the simulation. There is no termination in the algorithm: polymerization stops only when the program finds no further candidate pairs, either because the system is depleted in available monomers M or because the available monomers M are not in the vicinity of active units P*.

B. Step growth

Step growth is considered here in the case of a crosslinker X joining $E-P_n$ -E chains, where E stands for "end unit" and there are n repeat units within the chain. We consider only the reaction of the crosslinker at the end units. This is a representative situation for epoxy materials for instance, in which X is also called the *curing agent*, and is typical of step growth¹⁰.

The reaction mechanism is

$$E-P_n-E^{0*}+X^{s*} \xrightarrow{k} E-P_n-E^{1*}-X^{(s-1)*}$$
 (11)

in which the state of the left-end unit E is not relevant, it may be either free or already linked to a crosslinker. Here, X^{s*} is the *active* particle and E^{0*} the *target* particle. The crosslinker may have other bonds already, as long as s>0. The crosslinkers are given an initial state $s_0=f$ that corresponds to their chemical functionality f: the algorithm lets them form bonds up to f times. When s reaches 0, the algorithm stops the formation of further bonds.

An approximation for the kinetic evolution of the concentration of state s crosslinkers is

$$[X_0] = -k_0[X_0],$$
 (12a)

$$[\dot{X}_s] = -k_s[X_s] + k_{s-1}[X_{s-1}],$$
 (12b)

$$[\dot{X}_f] = k_{f-1}[X_{f-1}],$$
 (12c)

where Eq. (12b) is valid for 0 < s < f. k_s is the effective reaction rate that depends on k and on $\langle N_{X^sE^0} \rangle$

$$k_s = \langle N_{X^s E^0} \rangle k , \qquad (13)$$

where $\langle N_{X^sE^0} \rangle$ is the number of potential partners that may enter reaction (12); it will be determined by the radial distribution function later on. Results will be displayed with the number fractions of crosslinkers

$$x_s = \frac{[X_s]}{\sum_{s'=0}^f [X_{s'}]} \ . \tag{14}$$

Equation (12) is solved numerically with the routine odeint from SciPy¹¹ integrate module, using $x_0 = 1$ and $x_s = 0$ for the initial value.

The rate equation (12) provides a comparison point for the simulations, with the following limitations: (i) the equation neglects correlations in the system and (ii) it accounts for the structure only via the average values for $\langle N_{X^sE^0} \rangle$. The role of $\langle N_{X^sE^0} \rangle$ in the rate equation is to reproduce the steric hindrance around a crosslinker X: if X is already connected to f-s E particles, there is a corresponding lack of space for further E particles to connect to X.

C. Simulation details

To complete the bond formation model, we present here the Molecular Dynamics (MD) configuration with which the simulations of sections IV and V have been performed. All simulations are run using ESPResSo++⁷.

All the particles in the system have identical masses m and interact via a truncated Lennard-Jones 6-12 potential

$$V_{LJ}(r) = 4\epsilon \left(\left(\frac{\sigma}{r} \right)^{12} - \left(\frac{\sigma}{r} \right)^{6} + \frac{1}{4} \right)$$
for $r < \sigma_c$,
$$= 0 \text{ else.}$$
(15)

The ϵ and σ parameters are the same for all monomer and crosslinker particles. All quantities are reported in reduced Lennard-Jones units of mass m, length σ , energy ϵ and time $\sigma \sqrt{m \epsilon^{-1}}$.

Polymer chains in the step-growth simulations are held together by a FENE potential

$$V_F(r) = -\frac{1}{2}k_F R_0^2 \ln\left(1 - \left(\frac{r}{R_0}\right)^2\right)$$
 (16)

using the Kremer-Grest¹² parameters $k_F=30$ and $R_0=1.5$.

The bonds that are created during the simulations are modeled with a mirror Lennard-Jones potential² with the

same parameters as in Eq. (15):

$$V_b(r) = 4\epsilon \left(\left(\frac{\sigma}{2\sigma_c - r} \right)^{12} - \left(\frac{\sigma}{2\sigma_c - r} \right)^6 + \frac{1}{4} \right)$$
for $\sigma_c < r < 2\sigma_c$,
$$= 0 \quad \text{else.}$$
(17)

A velocity-Verlet integration with timestep $\Delta t = 0.0025$ is used for all simulations. A velocity rescaling thermostat is used to prepare the systems at temperature T=1. The number density is $\rho=0.8$. The thermostat is only used for the thermalisation of the system and is not necessary during the polymerisation part, due the the energy conservation property of the curing algorithm.

The simulations all follow the following protocol:

- Place particles at random in the simulation box. Chains for the step growth simulations are placed "one chain at a time" using the random-walk placement routine espresso.tools.topology.polymerRW of ESPResSo++.
- 2. Enable the thermostat.
- 3. Run a warmup integration in which the interaction potential are capped at a maximum value.
- 4. Run a warmup integration in which the interaction potential are uncapped.
- 5. Disable the thermostat.
- 6. Run the "production" run, with the polymerization mechanism enabled.

III. IMPLEMENTATION

The algorithm presented in Sec. II has been implemented in ESPResSo++⁷. ESPResSo++ is designed for extensibility at two levels: (i) the software is used by writing Python programs, in which it is possible to interact in a powerful manner with the system that is simulated and (ii) C++ extensions can be "plugged in" to modify the execution of the main simulation algorithms at many places. It is possible to add arbitrary operations at specific positions within the main MD looop.

We have written an extension, Association Reaction (or AR for short) that is executed within the Molecular Dynamics integrator, after the Velocity Verlet and thermostat have been run, i.e. it is connected to the aftIntV signal. The algorithm is run every Θ time steps. The specific value of Θ does not affect the result as it is taken into account in the acceptance criterion (4).

The behavior of the AR extension is influenced by the following parameters: the types of T and A, the minimum state for A s_{min}^A , δ T, δ A, the rate k, the interval Θ at which AR is run and the cutoff for the reaction.

TABLE I. Steps performed by the AssociationReaction extension. The lists used for storing the pairs and their contents at each steps are given. The presence of a Π indicates a parallel communication step.

Step	Action	List	Content
1.	Find all suitable candidate for a bond formation in the neighbor list of each particle.		
2.	Retain the candidates on the basis of a given rate, by comparing to a random number (see Eq. (4)).		
3.	Collect, for each A particle, the list of candidate targets T.	$L_{ m A}$	Local (id_A, id_T) pairs, ordered by id_A
4. Π	Consolidate the list among neighboring CPUs.	$L_{\rm A}$	Local and neighboring $(\mathrm{id}_A,\mathrm{id}_T)$ pairs, ordered by id_A
5.	Keep only one candidate pair per A particle	$L_{ m A}$	Unique (id_A, id_T) pairs, with respect to id_A
6. П	Assemble the candidate list for the target particles only.	L_{T}	Local and neighboring (id $_{\rm T}, \rm id_A)$ pairs, ordered by id $_{\rm T}$
7.	Select randomly, for each target particle, one activated particle.	L_{T}	Unique (id $_{\rm T}$,id $_{\rm A}$) pairs, with respect to id $_{\rm T}$
8. П	Communicate the selected pairs among neighboring CPUs.		
9.	For all the selected pairs: add the bond, modify the states for the active and the target particle.		

A. Parallel communication

In order to work in parallel, information on the bond choices must be communicated among neighboring processors. An important component of the implementation is the routine sendMultiMap that consolidates the candidate lists among neighboring CPUs and that is used three times for a reaction step (at each symbol Π in table I).

For the sake of clarity, the use of several terms is given in the context of parallel programming:

CPU: A processing unit that acts as a MPI worker.

neighboring CPU: A CPU that is in direct contact with a given one. Each CPU has 8 neighboring CPUs.

ghost: A ghost is a particle whose data is present on a CPU but for which the equations of motion are not solved. The presence of ghosts is necessary to compute force or reaction decisions.

We give here the explicit sequence of steps that are run by AR. The neighbors pairs are taken from the existing Verlet list that is used for the Lennard-Jones interaction. This convenience is possible because we select a cutoff for the reaction scheme that is the same as for the Lennard-Jones interaction. The communication pattern follows the implementation in storage::DomainDecomposition.

- For all neighbor pairs, collect the ones matching the type and state given as parameters as pairs (id_A, id_T).
- 2. Retain the matching pairs with rate k.

- 3. On each CPU, collect the pairs sorted by their id_A value in the list L_A .
- 4. Communicate $L_{\rm A}$ to all neighboring CPUs and merge the local and adjacent $L_{\rm A}$.
- 5. On the basis of $L_{\rm A}$, select only one T particle, at random, to react with each A. This choice is made on the CPU for which A is not a ghost.
- 6. Communicate $L_{\rm A}$ to all neighboring CPUs and merge the local and adjacent $L_{\rm A}$.
- 7. On the basis of $L_{\rm A}$, select only one A particle, at random, to react with each T, and collect them in the list $L_{\rm T}$.
- 8. Communicate $L_{\rm T}$ to all neighboring CPUs and merge the local and adjacent $L_{\rm T}$.
- 9. Apply the change to the states of the A and T particles from $L_{\rm T}$.

The algorithm is detailed in table I with the explicit mention of the communication steps and the content of the pair lists.

This algorithm ensures that each A or T particle can only participate in one new bond at each time step, even if several candidate bonds exist. This is achieved by selecting successively the pairs for a unique A and also for a unique T from the local and neighboring CPUs. The overall reaction rate depends naturally on the number of neighbor A T pairs in the system.

The effective bond formation is implemented by adding a bonded interaction term in the MD simulation. Explicitly, this amounts to call the add methods on the FixedPairList that contains the bonded Mirror Lennard-Jones interaction potential.

B. Current limitations

There are several possible extensions to the algorithm that would bring more generality. Taking into account several concurrent reactions is possible, following the Reactive multiparticle collision dynamics algorithm presented in Rohlf $et\ al\$ for collision-based hydrodynamical simulations. Further, the algorithm only considers irreversible reactions. Adding dissociation reactions would require an interaction potential that can be cut off without discontinuity. Quartic bonds have already been used for this purpose by Panico $et\ al^{13,14}$ in the LAMMPS¹⁵ Molecular Dynamics simulation code.

IV. SIMULATIONS OF CHAIN GROWTH

Simulations of chain growth start with N_{P^*} P* active units while the bulk of the simulation box is filled with monomer units M, for a total number of particles $N = N_{P^*} + N_M = 10^4$, the initial number fraction of polymer is equal to the concentration of active sites

$$\phi_0 = \frac{N_{P^*}}{N} \tag{18}$$

TABLE II. Parameters used for the simulations. C1 and C2 are the single and multiple chains growth simulations, respectively. S are the step growth simulations. The species A and T are integer indices corresponding to the particles type in ESPResSo++.

Run	A	δA	s_{min}^A	Т	δT	k	Θ	N_{tot}
C1	0	-1	2	0	1	1, 0.1 and 0.01	8	10000
C2	0	-1	2	0	1	0.1	80	10000
\mathbf{S}	1	-1	1	0	1	0.1 and 0.01	40	13500

The number of particles in the states M, P and P* is monitored for comparison with the rate equation. The resulting polymer fraction

$$\phi(t) = \frac{N_P + N_{P^*}}{N} \tag{19}$$

is then plotted for a proper comparison with the figures from Akkermans $et\ al^2$.

To obtain numerical data for $\langle N_{P^*M} \rangle$, for different chain lengths, simulations of single chains are run in which the growth is stopped when the polymer chain reaches n monomers. The integral of $g_{P^*M}(r)$ up to the cutoff radius is then used to obtain

$$\langle N_{P^*M} \rangle = \int_0^{r_c} 4\pi r^2 g_{P^*M}(r) dr \ .$$
 (20)

We observe a saturation of $\langle N_{P^*M} \rangle$ with the chain length and use this limit value to compute k_c .

The first simulations were performed with a single chain, for different rates k, and are displayed in Fig. 1.

As found by Akkermans $et\ al^2$, the rate equation only compares well for low values of k. When the reaction rate is too high, the active end of the chain is not given enough time to find a new partner by molecular diffusion.

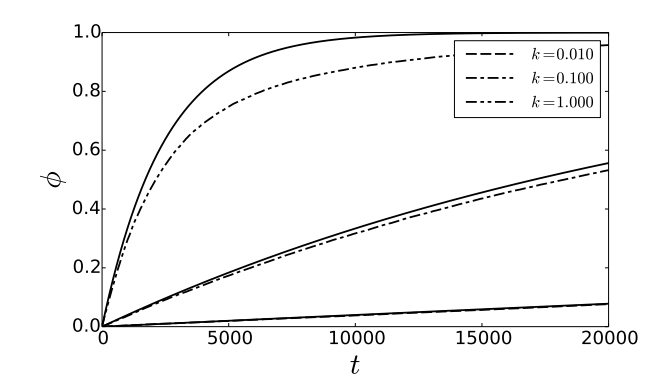


FIG. 1. Simulations of chain growth (dash-dotted curves), for a single chain, for different intrinsic rates k (see runs C1 of table II for the parameters). Each curve is the average over eight realizations. The full lines are the theoretical estimates for the corresponding effective rates from Eq. (10). For the fastest rate k=1 the theoretical estimates overestimates the monomer consumption rate, with respect to the simulation results. At lower rates the discrepancy is reduced.

To assess the behaviour of multiple chains growth, corresponding simulations have been run with initial polymer fractions ϕ_0 of 1, 3, 5, 10, 15 and 20 10^{-3} . The resulting $\phi(t)$ is displayed as a fraction of the scaled time $k_c[P^*]t$ in Fig. 2.

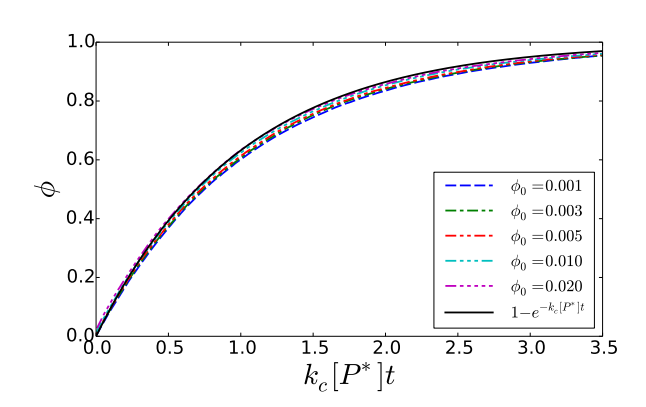


FIG. 2. Simulations of chain growth for multiple chains, for initial polymer fractions $\phi_0 = 1, 3, 5, 10, 15$ and $20 \ 10^{-3}$ and rate k = 0.1 (see runs C2 of table II for the parameters). The time is rescaled by the effective rate $k_c[P^*]$ so that the theoretical estimate (full line) matches all simulation data.

Given enough time, all chain growth simulations were observed to approach $\phi=1$, similarly to the limit of Eq. (10).

V. SIMULATIONS OF STEP GROWTH

We have performed simulations of step growth of a model system consisting of polymer chains $E-(P)_n-E$ with n=3, thus consisting of five monomer units, and of crosslinkers X^f . The simulations have been run with f=0,1,2,3,4,5 and rate k=0.1 and 0.1 for a system of 2500 chains $E-(P)_3-E$ and 1000 crosslinkers X, for a total of 13500 particles in the system. These parameters give a stoechiometric ratio for f=5. They have been used for all values of f to have only a single parameter vary across the simulations.

First, the radial distribution function $g_{X^sE^0}(r)$ between the crosslinker X^{s*} and available end-unit E^{0*} has been computed from simulations with f=0,1,2,3,4 and 5, and k=0.1, where the polymerization runs for 5000 time units and is then stopped. The sampling for $g_{X^sE^0}(r)$ is done for 5000 subsequent time steps. The integral of $g_{X^sE^0}(r)$ up to the cutoff radius is then used to obtain

$$\langle N_{X^s E^0} \rangle = \int_0^{r_c} 4\pi r^2 g_{X^s E^0}(r) dr \ .$$
 (21)

The values of $\langle N_{X^sE^0} \rangle$ are given in Table III for reference.

TABLE III. The average number of available neighbors for curing in the step-growth simulations.

Then, the polymerization has been studied in simulations where two rates have been used, k=0.1 and 0.01 and the results are shown in Fig. 3.

For low functionality (f=1 or 2), the concentrations $[X^{s*}]$ given by Eqs. (12) compare well to the ones from the simulations. The simulation data shows a delay in the polymerization process, with respect to the rate equation, similarly to what has been observed for chain growth (see Sec. IV). For higher functionality, the rate equation compares well to the simulation data only for the initial stages of the polymerization. Results for kt up to 1.5 are displayed to highlight the proper capture of the initial polymerization kinetics.

The discrepancy between the rate equation and the simulation data is unavoidable, as the rate equation only considers the average value for the number of reaction candidates, and highlights a motivation to develop the full simulation model.

Figure 4 presents the same data as Fig. 3 with a larger time span (for f = 4 and f = 5 only). For f = 4, the fraction x_4 of fully crosslinked X particles saturates at 1 (maximum value), similarly to the kinetic model. For f = 5, besides the observed lag in the polymerization, we observe that x_5 does not reach the same saturation value. Indeed, crosslinkers having already formed four

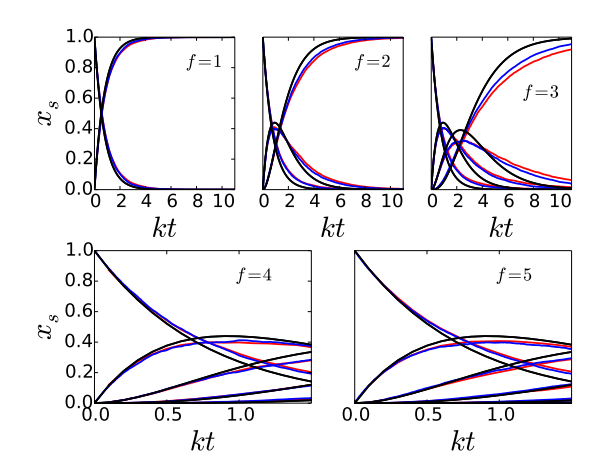


FIG. 3. Concentration of crosslinker states for the step-growth simulations with f=1,2,3,4 and 5. The full black lines are obtained from Eqs. (12), and the full red and blue lines come from simulation with k=0.1 and k=0.01, respectively. Each simulation result is the average over eight realizations. See the parameters for runs S in table II. The curves starting at $x_s=1$ correspond to x_0 . The curves starting at x_s correspond x_s with $x_s>0$, where the curves growing faster initially correspond to a lower $x_s=1$ (the fastest growing curve is for $x_s=1$, and so on). For $x_s=1$ and $x_s=1$ 0, the rate equation captures properly the evolution of crosslinking. For higher functionalities, it fails to track the quantitative evolution beyond $x_s=1$ 0.

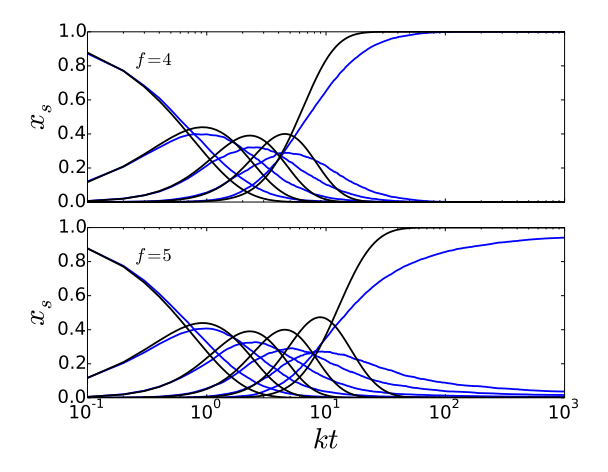


FIG. 4. Same data as in Fig. 3 for k=0.1 and f=4 and 5, with a logarithmic axis for the time (x-axis). Data is shown up to the end of the simulation, to highlight the saturation of x_5 (bottom panel) below the limiting value of 1 that is reached for f=4 (top panel).

bonds (in the case f=5) have on average 0.01 neighbours. This average hides the fact that many of these crosslinkers have zero neighbors of type and state E^{0*}

that would allow further reaction. The polymerization is thus stopped by an effective depletion of reactant.

VI. CONCLUSIONS

We have presented an adaptable algorithm for thermoneutral polymerization in parallel Molecular Dynamics (MD) simulations. The algorithm handles several polymerization mechanisms and may involve molecular compounds in which only selected sites participate in the polymerization process, as was done here for step growth.

The kinetic model of Akkermans $et\ al^2$ was validated on the chain growth results and a kinetic model for step growth was introduced and compared favorably to the simulations. A systematic delay of the simulation process in the simulation is found for both growth mechanisms. That delay was also found in Refs. 2 and 3 and is caused by the simplifications made in the rate equations with respect to the full molecular simulations.

Due to the relative simplicity of coarse-grained models, with respect to atomistic descriptions, it is possible to control the polymerization process in its time evolution and to avoid typical artifacts such as energy jumps and discontinuous trajectories. On the basis of the present work, it is possible to backmap a system's coordinates to the atomistic level after the polymerization process. Several extensions of the algorithm are feasible: introduce several concurrent chemical reactions with different intrinsic rates or further constrain the reaction acceptance to conformation properties (e.g. to avoid unrealistic angles in the newly formed molecule).

While the present work is limited to irreversible reactions, other works have already considered interaction potentials than "break" past a given cutoff¹³. An alternative approach to the dissociation process is to consider a stochastic rate at which a bond dissapears¹⁶. This latter approach does not achieve energy conservation however. No solution that combines continuous trajectories

and stochastic dissociation has been proposed yet.

ACKNOWLEDGMENTS

The authors acknowledge fruitful interactions with the developers of ESPResSo++. This work was supported by the "Strategic Initiative Materials" in Flanders (SIM) under the InterPoCo program. The computational resources and services used in this work were provided by the VSC (Flemish Supercomputer Center), funded by the Hercules Foundation and the Flemish Government – department EWI.

- ¹D. Frenkel and B. Smit, *Understanding molecular simulation:* from algorithms to applications (Academic press, 2001).
- ²R. L. C. Akkermans, S. Toxvaerd, and W. J. Briels, J. Chem. Phys. **109**, 2929 (1998).
- ³R. S. Hoy and G. H. Fredrickson, J. Chem. Phys. **131**, 224902 (2009).
- ⁴K. Tucci and R. Kapral, J. Chem. Phys. **120**, 8262 (2004).
- ⁵K. Rohlf, S. Fraser, and R. Kapral, Comput. Phys. Commun. 179, 132 (2008).
- ⁶M. F. Russo Jr. and A. C. van Duin, Nucl. Instrum. Methods Phys. Res. Sect. B **269**, 1549 (2011), computer Simulations of Radiation Effects in Solids.
- ⁷J. D. Halverson, T. Brandes, O. Lenz, A. Arnold, S. Bevc, V. Starchenko, K. Kremer, T. Stuehn, and D. Reith, Comput. Phys. Commun. **184**, 1129 (2013).
- ⁸D. Mukherji and C. F. Abrams, Phys. Rev. E **79**, 061802 (2009). ⁹Boost C++ Libraries, http://www.boost.org/.
- ¹⁰M. P. Stevens, *Polymer Chemistry* (Oxford University Press, 1999).
- ¹¹E. Jones, T. Oliphant, P. Peterson, et al., "SciPy: Open source scientific tools for Python," (2001–).
- ¹²K. Kremer and G. S. Grest, J. Chem. Phys. **92**, 5057 (1990).
- ¹³M. Tsige and M. J. Stevens, Macromolecules **37**, 630 (2004).
- ¹⁴M. Panico, S. Narayanan, and L. C. Brinson, Modelling Simul. Mater. Sci. Eng. 18, 055005 (2010).
- ¹⁵S. Plimpton, J. Comput. Phys. **117**, 1 (1995).
- ¹⁶M. Caby, P. Hardas, S. Ramachandran, and J.-P. Ryckaert, J. Chem. Phys. **136**, 114901 (2012).